Full Length Article

Development of a kinetic approach for the liquid phase dehydrogenation of perhydro benzyltoluene

T. Mader [a,b], M. Blasius [a,b], S. Pappler [a,b], T. Rüde [a], M. Geißelbrecht [a], P. Wasserscheid [a,b,c,*]

[a] Forschungszentrum Jülich, Helmholtz-Institute Erlangen-Nürnberg for Renewable Energy (IET 2), Cauerstraße 1, 91058 Erlangen, Germany
[b] Lehrstuhl für Chemische Reaktionstechnik, Friedrich-Alexander-Universität Erlangen-Nürnberg, Egerlandstr. 3, 91058 Erlangen, Germany
[c] Forschungszentrum Jülich, Institute for a Sustainable Hydrogen Economy, Marie-Curie-Straße 5, 52428 Jülich, Germany

ABSTRACT

This publication examines the dependency of the liquid phase dehydrogenation of perhydro-benzyltoluene (H12-BT) on process parameters like temperature, pressure and LOHC concentration, to develop a kinetic approach for a commercial dehydrogenation catalyst. The investigations revealed that the commercial pellet catalyst is limited by pore diffusion. Therefore, the catalyst was milled to study the intrinsic reaction rate. The investigations were used to develop both an intrinsic and an effective kinetic approach to describe the dehydrogenation of H12-BT. The kinetic approach developed in this work describes for the first time the liquid phase dehydrogenation of H12-BT considering the dependency of the reaction rate on the hydrogen partial pressure, and the limitation due to thermodynamic equilibrium. Additionally, the influence of reactant and product concentration and the concentration of the main intermediate is considered in the developed kinetic approach. Based on both kinetic approaches, the utilization of the catalyst is calculated and found to be below 50% under technically relevant conditions. The study therefore demonstrates the significant potential to optimize the catalyst in the future, as currently only part of the expensive platinum is being used effectively. The developed kinetic approaches provide the basis for future modelling of a dehydrogenation reactor.

1. Introduction

Liquid Organic Hydrogen Carriers (LOHC) have emerged as a promising solution for hydrogen storage as they enable safe and effective hydrogen storage at ambient conditions. Hydrogen reversibly reacts in an exothermal and heterogeneously catalyzed hydrogenation with a hydrogen-lean molecule to form a hydrogen-rich molecule that is liquid at ambient conditions. As the stored hydrogen is chemically bound to the carrier molecule, no molecular hydrogen is present at the time of hydrogen storage or transportation. The stored hydrogen can be released in an endothermal and heterogeneously catalyzed dehydrogenation reaction from the hydrogen-rich molecule. This conversion step leads to the reformation of the hydrogen-lean carrier to close the storage cycle [1–5]. If the LOHC system involves only hydrocarbons, repurposing of the current infrastructure for the distribution of liquid hydrocarbons is possible. This avoids cost for establishing new infrastructures and may fasten the start-up of a global hydrogen economy. Additionally, heavy-duty mobility is an emerging market for hydrogen or hydrogen derivatives as many types of heavy-duty vehicles cannot be fully electrified with batteries. LOHCs are recently discussed as promising fuels for on-board hydrogen supply of heavy-duty vehicles [6,7].

The three most promising and most investigated pure hydrocarbon LOHC systems are: Toluene (TOL)/ methylcyclohexane (MCH) [8–10], perhydro dibenzyltoluene (H18-DBT)/ dibenzyltoluene (H0-DBT)/ [11–13], and perhydro benzyltoluene (H12-BT)/ benzyltoluene (H0-BT) [4,12–15]. A detailed comparison of these different systems can be found in Rüde et al. [2]. The H12-BT/H0-BT system combines some of the advantages of TOL/ MCH (low viscosity and fast pore diffusion in catalytic transformations) with the advantages of H18-DBT/H0-DBT (high density leading to high volumetric storage density, low vapor pressure). Additionally, the hydrogenation and dehydrogenation of H12–BT/ H0-BT is faster and more selective than the respective reactions in the H18-DBT/H0-DBT system. The H0-BT/H12-BT system is used in this study because of these technical relevant advantages.

The dehydrogenation of H12-BT is catalyzed by platinum nanoparticles supported on porous alumina supports. Current catalyst development studies focus on the variation of the size of the platinum nanoparticles [16], the acidity of the support surface [17], and the textural properties of the support [18]. Furthermore, bimetallic catalyst impregnations or doping of the Pt nanoparticles with small amounts of sulfur has been shown to enhance productivity and selectivity of the H12-BT dehydrogenation catalyst considerably [19,20].

The dehydrogenation of H12-BT is a consecutive reaction that involves formation of the intermediate H6-BT. The latter releases further hydrogen to form H0-BT as shown in Fig. 1 [2].

The degree of hydrogenation (DoH) is defined as the actual amount of hydrogen reversibly bound in a given hydrogen carrier divided by the maximum amount of hydrogen that can be stored reversibly. The definition of the DoH is given in Eq. (1). The DoH is an important parameter describing the utilization of the carrier's hydrogen capacity. Process conditions are chosen in the hydrogenation step to maximize the DoH in the LOHC system at hand. Hydrogen release, in contrast, aims for the lowest possible DoH to make as much hydrogen available for a given application as possible.

$$DoH = \frac{n_{H2,stored}}{n_{H2,max}} = \frac{\frac{n_{H6-BT}}{2} + n_{H12-BT}}{n_{H0-BT} + n_{H6-BT} + n_{H12-BT}} \quad (1)$$

How to determine the optimal process conditions to operate the H12-BT/H6-BT/H0-BT LOHC system? Here, both thermodynamic and kinetic aspects have to be considered. Rüde et al. experimentally determined the DoH at thermodynamic equilibrium using a pressure swing reactor [2]. They employed a sigmoidal function to describe DoH as a function of temperature and total pressure. Bong et al. [21] have described the thermodynamic equilibrium in the H12-BT/H6-BT/H0-BT LOHC system based on Gibbs free energies [21].

However, most published studies on H12-BT dehydrogenation [15–17] do not aim for reaching equilibrium DoH values. Instead, these studies target a more detailed understanding of the dehydrogenation kinetics to enable the proper design of dehydrogenation reactors or an accurate prediction of the quantity of released hydrogen under given conditions. The development of suitable kinetic models is particularly important in this context. The H18-DBT/H0-DBT shows similarities to the H12-BT/H0-BT system as H18-DBT dehydrogenation is also conducted under multiphasic conditions with several intermediates. Therefore, established kinetic models of H18-DBT dehydrogenation are firstly discussed to transfer the findings to the dehydrogenation of H12-BT. Park et al. [22] used a power-law approach to describe the reaction rate of the dehydrogenation of H18-DBT in the temperature range between 270 and 320 °C. The concentration variation of the feed was achieved by mixing H18–DBT and H0-DBT. This is a simple approach to mimic different DOHs in the feedstock. It is however known that the desorption of the H12-DBT and H6-DBT rection intermediates is very different from the desorption of H0-DBT from the catalyst surface. Therefore the study of H18-DBT/H0-DBT mixtures may not be representative for a real reaction mixture with the same formal DoH [23]. The reported kinetic approach by Park et al. [22] also neglect pressure dependencies and the effect of thermodynamic limitations on the reaction rate, i.e. for each temperature the model results converge to full hydrogen release despite the known thermodynamic limits relevant for the applied conditions [24]. Geißelbrecht et al. [11] used a power law approach to describe dehydrogenation of H18-DBT with considering thermodynamic limitations.

Hydrogen release studies from H12-BT aiming at the development of kinetic models have been carried out by Rüde et al. [25]. The authors also described the reaction by a simple power law approach neglecting the intermediate H6-BT. No thermodynamic limitations were considered in their approach because their special use case of a catalytic distillation represents an open system, where H0-BT and hydrogen is constantly removed from the catalyst-filled reaction volume [25]. Wang et al. [14] developed a kinetic approach for H12-BT dehydrogenation considering the intermediate H6-BT. They used a commercially available cylindrical granular catalyst from Thermo Fisher containing 5.0 wt% Pt on Al$_2$O$_3$ for their investigations. The experiments were conducted in a temperature range between 250 and 265 °C as higher temperatures were not accessible due to the evaporation of the reaction mixture with undefined hydrogen content (Hx-BT) in their atmospheric pressure setup. For the same reason, no pressure variation was performed. Wang et al. [14] fitted their experimental data to a power law and a Langmuir-Hinshelwood-Hougen-Watson (LHHW) approach. The LHWM approach was found to offer a higher accuracy compared to the power-law model, which is mainly due to the higher amount of fitting parameters. The H12-BT dehydrogenation was described as slurry phase reaction (solid catalyst in liquid H12-BT) as the influence of Hx-BT evaporation was limited by recondensation of the evaporated Hx-BT.

Slurry phase H12-BT dehydrogenation offers some interesting advantages over performing the same reaction with evaporated H12-BT in gas/solid contact: i) The liquid LOHC phase surrounding the catalyst can dissolve coke precursors from the catalyst surface thus preventing their further growth to deactivating coke [26], as a result the catalyst operation time can be significantly extended [27]; ii) heat transfer to the catalyst bed to compensate for the heat consumption by the endothermal dehydrogenation reaction is improved in the presence of liquid that acts as heat transfer medium from the hot reactor walls to the reaction site, better heat transfer leads to higher average temperatures in the catalyst bed and higher reaction rates [15,28].

To ensure slurry phase operation in the dehydrogenation reactor, H12-BT must be fed into the reactor in liquid form, and the total pressure in the dehydrogenation reactor must be high enough to keep part of the Hx-BT in the liquid phase at the given temperature, even if the thermodynamically maximum possible amount of hydrogen is released. However, increasing the pressure limits the achievable conversion in H12-BT resp. H6 BT dehydrogenation. So, the choice of reaction conditions is a compromise between enabling good dehydrogenation kinetics and thermodynamic and ensuring longevity of the catalyst and good heat transfer. Maximizing the hydrogen release is necessary in order to fully exploit the hydrogen storage capacity of the H12-BT molecule.

In this contribution, we present a kinetic model for the slurry phase dehydrogenation of H12-BT using the commercial catalyst EleMax D102 of Clariant which is an egg-shell impregnated, sulfur-doped platinum catalyst (loading 0.3 mass% Pt) on a neutral alumina. Table S1 shows the properties of the commercial catalyst, which are not banned from publication.

To develop an intrinsic model, we had to ensure that the determined reaction rate is not influenced by internal or external mass transfer limitations. Therefore, our kinetic experiments are carried out with crushed catalyst powder of defined size. Our kinetic approach considers
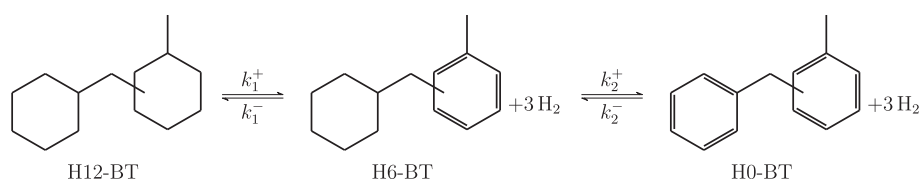

Fig. 1. Main dehydrogenation/hydrogenation reactions in the LOHC system H12-BT/H6-BT/H0-BT.

the consecutive reaction from H12-BT to H6–BT and from H6-BT to H0-BT. Moreover, we are considering limitations by the thermodynamic equilibrium in our approach. In addition, we have studied dehydrogenation kinetics with the commercial catalyst pellets where internal diffusion effects play a role. Based on our data and derived models for both catalyst materials we can estimate the effect of pore diffusion on the observed dehydrogenation kinetics for the commercial pellets catalyst and can indicate the effectiveness factor of the pelletized commercial catalyst.

2. Experimental

2.1. H12-BT dehydrogenation in a Semi-Batch-Autoclave

All dehydrogenation experiments were conducted in a high temperature, high pressure autoclave of Parr Instruments (Type 4575A, 500 ml volume). The operation of the autoclave has been described in various publications [2,24,27]. The autoclave was equipped with a heating jacket and an internal cooling coil. Moreover, temperature and stirring speed were controlled via a Parr Controller (Type 4848). A backpressure regulator from Equilibar was used to set the desired reaction pressure. The temperature of the reflux condenser was set to 1 °C to prevent evaporated Hx-BT from leaving the reactor. All experiments were carried out with H12-BT purchased from Hydrogenious LOHC Technologies GmbH. The used catalyst was the EleMax D102 from Clariant (loading 0.3 mass% Pt and material number 309080), which comes in the form of spherical catalyst pellets with an average diameter of 3 mm. For the variation of the particle size the catalyst was milled and sieved to realize different catalyst particle sizes. The platinum content of each size fraction was determined by ICP-OES. The platinum concentration slightly increased with decreasing particle size of the catalyst. However, the ratio of platinum to H12-BT was kept constant over all experiments considering the different platinum concentration in each size fraction. The specific surface area of the milled catalysts was determined and did not change as a result of the milling process.

After filling the reactor with H12-BT (300 g, DoH = 0.97) and catalyst, the system was flushed with nitrogen to remove any oxygen. Afterwards, the reactor was flushed with hydrogen to remove the nitrogen. Before heating, the reactor was pressurized with 9 bara hydrogen to prevent any hydrogen release from the H12-BT in the startup phase. To exclude hydrogen release in the startup-phase, a sample was taken after each startup phase and analyzed via GC. The sample showed no difference to the used H12-BT feedstock and thus dehydrogenation activity in the startup phase can be excluded. The reaction was started by lowering the reactor pressure to the desired operating pressure. The total pressure remained constant throughout the experiment. The hydrogen partial pressure was calculated at the start of the reaction based on the actual DoH of the Hx-BT mixture. Due to the slightly decreasing vapor pressures with decreasing DoH, the hydrogen partial pressure increases during the reaction despite the constant absolute pressure, a fact that is considered in our model. Throughout the experiment, liquid samples were taken, to analyze the DoH using a standard GC procedure that was previously published [19]. The mass losses due to sampling are considered in our mass balance calculations.

The shaped catalyst was placed directly in the reactor without using a catalyst basket. After each experiment we checked for signs of catalyst abrasion. But this was not found to be a relevant concern. The amount of milled catalyst used in the kinetic experiments was 1.78 g, resulting in a Pt-to-LOHC ratio of 1:57135. In comparison, 4.52 g of the pelletized catalyst was used, corresponding to a Pt-to-LOHC ratio of 1:22050.

2.2. Determination of the reaction equilibrium

The aim of this work was to determine the reaction kinetics for the dehydrogenation of H12-BT and H6-BT. For thermodynamic reasons, full conversion is not possible for all process parameters, so the influence

of the equilibrium must be considered in our model. It was decided not to use the equilibrium data from Rüde et al. [2] because they neglect the presence of the intermediate H6-BT. Instead, the thermodynamic equilibrium is described by the calculation of Gibbs free energy. We have adapted the calculation procedure for the equilibrium constant from Heublin et al., who have described the procedure in detail for the liquid phase dehydrogenation of N-ethylcarbazole [29]. The thermodynamic equilibrium is reached when the Gibbs free energy is at a minimum. The equilibrium constant K_{eq} can be calculated using Eq. (2), neglecting activity coefficients, assuming ideal gas behavior, and a reaction occurring exclusively in the liquid phase.

$$K_{eq} = \exp\left(\frac{-\Delta g_r^0}{RT}\right) = \frac{x_{Product}}{x_{Educt}} \left(\frac{p_{H2}}{p^\theta}\right)^{\sum \nu_{H2}} \tag{2}$$

The Gibbs free enthalpy is calculated using Eq. (3).

$$\Delta g_r^0 = \Delta h_r^0 - T\Delta s_r^0 \tag{3}$$

The reaction enthalpy equals the sum of the standard formation enthalpies of all reactants multiplied by the stoichiometric coefficients. The reaction entropy equals the sum of the standard molar entropies of all reactants multiplied by the stoichiometric coefficients. The gas phase standard formation enthalpies for the reactants are given in the NIST database [30]. Since the liquid phase standard formation enthalpies are required, the gas phase standard formation enthalpies can be converted in the liquid phase formation enthalpies using the evaporation enthalpies reported from Vervekin et al. [31]. The temperature dependence of the standard formation enthalpy was neglected in our calculations. The gas phase reaction entropies are listed in the NIST database [30]. The gas phase reaction entropies were converted in liquid phase reaction entropies using the Pictet-Trouton rule and the evaporation enthalpy reported by Vervekin et al. [31]. We have used the Van't Hoff Eq. to describe the temperature dependency of the equilibrium constant K_{eq}. The reaction enthalpy was assumed to be constant for all process conditions.

The composition of the gas phase was calculated using the vapor–liquid-equilibrium (VLE). We have neglected the solubility of hydrogen in liquid Hx-BT mixture, because the solubility is very small due to the relatively low total pressure [21]. The vapor pressure of H12-BT was taken from Jorschick et al. [32], and the vapor pressure of H0-BT was taken from the manufacturer's data sheet [33].

The only available vapor pressure data for H6-BT was published by Verevkin et al. [31]. The vapor pressure was determined in the temperature range between 45 and 85 °C. Extrapolation of the data to the reaction temperature of around 300 °C is associated with a significant uncertainty. Instead, we have first estimated the vapor pressure of H6-BT. Then, the ratio of $p_{H12-BT,lv}$ to $p_{H6-BT,lv}$ was calculated in the temperature range measured by Verevkin et al. [31]. Finally, this ratio was taken as a constant and transferred to the vapor pressure data of Jorschik et al. [34]. The temperature dependency of the equilibrium constants is shown in Fig. S2. In general, the dehydrogenation of H12-BT is thermodynamically much more favored than the dehydrogenation of H6-BT.

3. Results and discussion

The dehydrogenation of H12-BT is a multiphasic reaction catalyzed by a heterogeneous catalyst. To develop an intrinsic kinetic approach limitations by internal and external mass transfer must be excluded. [35] The reproducibility of the experimental setup was checked for a representative experiment, and the results are shown in Fig. S3.

3.1. Influence of external mass transfer

The external mass transfer depends on the thickness of the laminar boundary layer around the catalyst. The thickness of the laminar boundary layer decreases with increasing flow velocity, which in our

case is governed by the stirring rate. External mass transfer limitations can therefore be excluded if the reaction rate does not increase with higher stirring rates. The influence of the stirring rate on the progress of the DoH is shown in Fig. 2. Fig. 2A shows the influence of the stirring rate on the pellet catalyst and Fig. 2B reveals the influence on the milled catalyst (< 250 μm). The dedicated graphical representation of the molar substance quantities can be found in the supplementary information S4 and S5. No significant change in the reaction rate is observed for a stirring rate above 250 min^{-1} for the pellet catalyst. So, limitations by external mass transfer can be excluded for the pellet catalyst at a stirring rate above 250 min^{-1}. To not falsify the experiment by an undetected change in pellet geometry, the catalyst was checked for abrasion after each experiment and no significant abrasion of the pellet was detected. For further experiments with pellet catalysts, a stirring rate of 400 min^{-1} is chosen. For the milled catalyst no increase in the reaction rate is detected for a stirring rate above 800 min^{-1}. Therefore, a stirring rate of 1,000 min^{-1} is chosen for further experiments with milled catalyst. The need for a higher stirring rate in experiments with the milled catalysts is probably not caused by the size of the laminar boundary layer but is to avoid settling of the milled catalyst. Settling reduces the dispersion of the catalyst in the reactor and thereby complicates the mass transfer of the reactants to the catalyst active sites.

3.2. Influence of internal mass transfer

Limitation of the observable rate by internal mass transfer occurs if the rate of the surface reaction is higher than the pore diffusion rate of the reactants. The internal diffusion rate can be increased at constant reaction conditions if the critical pathway of diffusion is reduced, e.g. by using pellets with a smaller diameter. The rate of the surface reaction, in contrast, is not influenced by the particle size of the catalyst. Therefore, an increasing observable rate with decreasing catalyst particle size indicates rate limitation by pore diffusion effects. Conversely, if the observable rate of reaction stays constant with decreasing catalyst pellet size intrinsic reaction rates can be measured.

Fig. 3 shows a variation of the catalyst particle size at 310 °C. The evaluation was purposely carried out at the highest temperature considered in our study because the reaction rate of the surface reaction has a higher dependency on temperature than the internal diffusion rate. The graphical representation of all molar substance quantities can be found in the ESI (Fig. S6).

We found that all milled catalyst materials show a significantly faster hydrogen release compared to the pelletized catalyst. This means that the activity of the pelletized catalyst is influenced by pore diffusion effects. However, no further increase in reaction rate was observed when
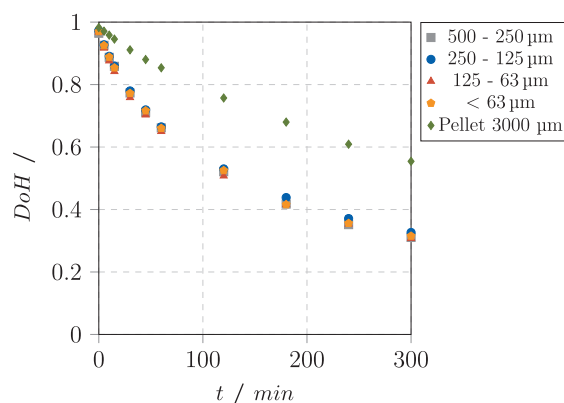
Fig. 3. Effect of the particle size on the reaction rate, Pt to LOHC-Ratio: 1/57135, 310 °C and 4 bara.

the particle size of the ground catalyst was further reduced to less than 500 μm. This suggests that pore diffusion effects do not occur at catalyst particle sizes below 500 μm. For our kinetic experiments, we used particle sizes of < 250 μm to remain safely within the range of intrinsic kinetics.

3.3. Intrinsic reaction rate

With this experimental procedure suitable for the determination of intrinsic kinetics we studied systematically the H12-BT dehydrogenation reaction in order to determine intrinsic reaction rates as a function of temperature, reaction pressure and the concentration of the LOHC species (H12-BT, H6–BT and H0-BT).

3.3.1. Dependency on temperature

Fig. 4 shows the dependency of the intrinsic reaction rate on temperature (between 270 and 320 °C) at an initial hydrogen partial pressure of 1.7 bara. Note that the total pressure in the reactor had to be adjusted with increasing temperature to compensate for the increase in H12-BT vapor pressure with rising temperatures. The hydrogen partial pressure increases with reaction progress as H0-BT has a lower vapor pressure than H12-BT and the total pressure is constant.

At 270 °C hardly any hydrogen release is detected. Hydrogen release increases significantly with rising temperature. Since H6-BT is an intermediate, it is produced by the dehydrogenation of H12-BT and consumed by further dehydrogenation to H0-BT. The maximum H6-BT concentration is more quickly reached for higher reaction temperatures.
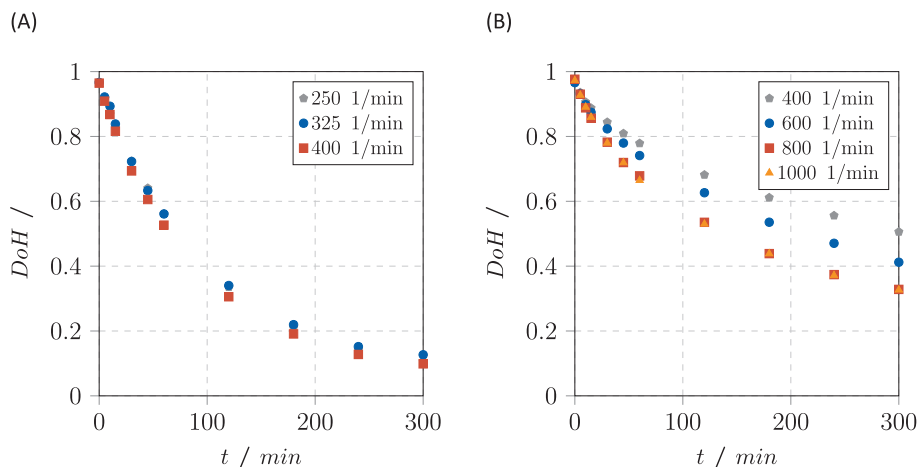
(A)

(B)

Fig. 2. Effect of stirring rate on reaction rate: (A) Pellets, Pt to LOHC-Ratio: 1/22050, 320 °C and 4 bara, and (B) milled catalyst powder, < 250 μm, Pt to LOHC −Ratio: 1/57135, 310 °C and 4 bara.
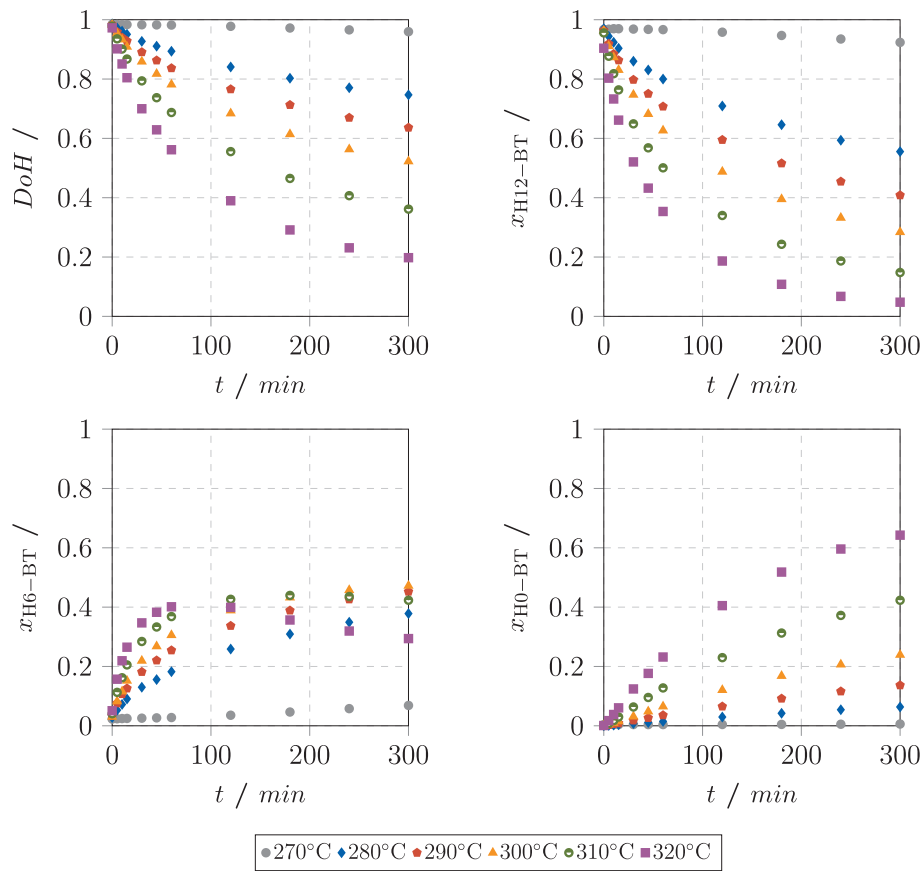
Fig. 4. Effect of reaction temperature on the intrinsic reaction rate at a constant hydrogen partial pressure of 1.7 bara. Pt to LOHC-Ratio: 1/57135, powder catalyst < 250 μm, 270 – 320 °C, 2.8 – 4.7 bara and stirring rate of 1000 1/min.

3.3.2. Dependency on pressure

Fig. 5 shows the influence of the hydrogen partial pressure on the reaction rate at a constant reaction temperature. It is found that the hydrogen release far away from the thermodynamic equilibrium is only slightly influenced by the hydrogen partial pressure. Interestingly, a somewhat larger influence of the hydrogen partial pressure variation on H0-BT formation is observed compared to the influence on H6-BT formation.

Note that the pressure dependency of H12-BT dehydrogenation is more pronounced in this study than in previously published continuous dehydrogenation experiments 12, 15]. This is understandable from the fact that in these batch autoclave experiments all evaporated Hx-BT species are recondensed and transferred back to the reactor. Additionally, complete wetting of the catalyst is ensured by fast removal of the released hydrogen from the liquid phase. In contrast, the results in the previously published continuous H12-BT dehydrogenation experiments always reflected a complex interplay of catalytic surface reaction, Hx-BT evaporation and catalyst wetting.

3.3.3. Parameter estimation

A simple but commonly used approach to describe the reaction rate in heterogeneously catalyzed reactions is the power law approach [36–38]. As complete hydrogen release is thermodynamically not possible under all considered process conditions, a power law approach including thermodynamic limitations has been chosen. Most frequently the rate constant of the reverse reaction is expressed as the ratio of the forward rate constant $k_{0,i}$ and the equilibrium constant K_{eq}. The equilibrium constant can be described based on physical parameters of the species involved and so the amount of fitting parameters is reduced. As we have seen a clear dependency of the reaction rate on the hydrogen partial pressure, we are also considering hydrogen partial pressure as a

parameter in our kinetic approach. As shown in Fig. 1, we are considering two consecutive reactions to describe H12-BT/ H6–BT dehydrogenation. Therefore, we must estimate the parameters for two individual reaction rates representing the dehydrogenations of H12–BT (Eq. (4)) and H6-BT (Eq. (5)), respectively.

$$r_{1,m} = k_{0,1} \cdot exp\left(-\frac{E_{A,1}}{R \cdot T}\right) \cdot C_{H12}^{a1} \cdot p_{H2}^{a2} \cdot \left(1 - \frac{C_{H6} \bullet \left(\frac{p_{H2}}{p^{\varnothing}}\right)^3}{K_{eq,1} \cdot C_{H12}}\right) \quad (4)$$

$$r_{2,m} = k_{0,2} \cdot exp\left(-\frac{E_{A,2}}{R \cdot T}\right) \cdot C_{H6}^{b1} \cdot p_{H2}^{b2} \cdot \left(1 - \frac{C_{H0} \bullet \left(\frac{p_{H2}}{p^{\varnothing}}\right)^3}{K_{eq,2} \cdot C_{H6}}\right) \quad (5)$$

The parameter $p^{\varnothing}$ is the reference pressure and was chosen to be 1 bar. To calculate the reaction rate from the concentration curves, the system of ordinary differential equations was solved using the ODE15s solver in the Matlab software. The model parameters were estimated by fitting the experimental data using MATLAB's lsqcurvefit function with the trust-region-reflective algorithm. To minimize the risk of converging to a local minimum, the MultiStart-function was applied, systematically varying the initial conditions across a broad parameter space. Since multiple solver runs consistently converged to the same minimum, we assume that the global optimum was identified. The estimated parameters are summarized in Table 1 for the case of the ground powder catalyst.

The activation energy for both individual reactions is between 140 and 150 kJ mol^{-1}. The activation energy estimated in our study is significantly higher than the activation energy estimated by Wang et al.
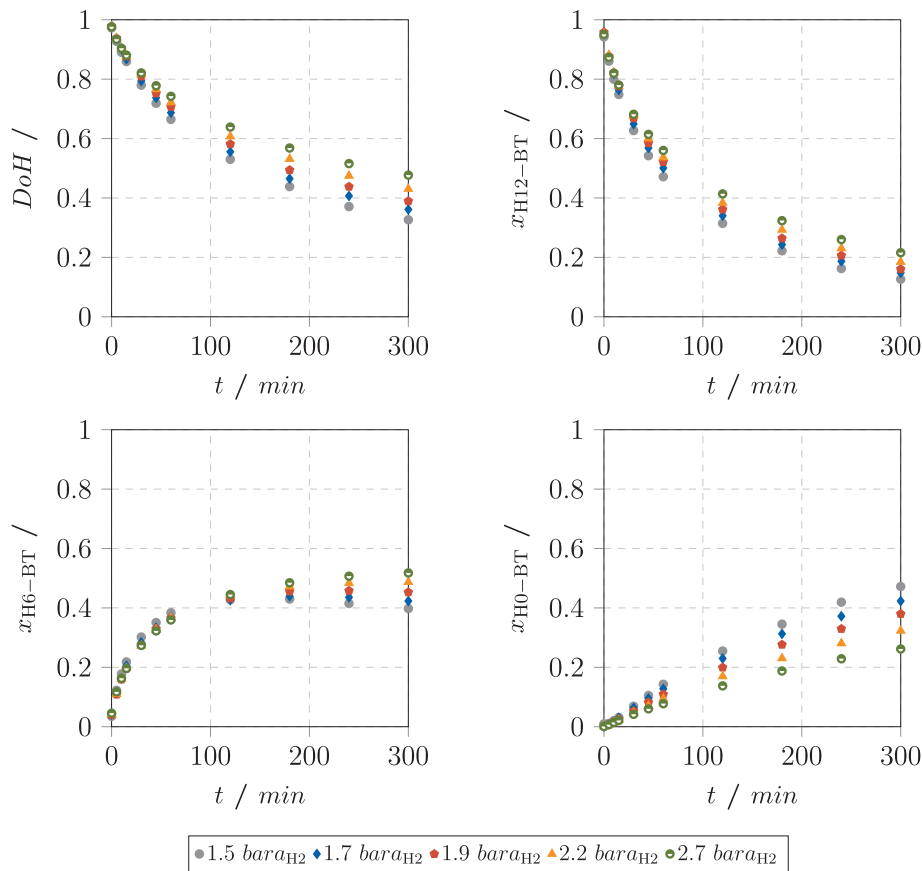
Fig. 5. Effect of the hydrogen partial pressure on DOH over time and consumption/formation of H12-BT, H6-BT and H0-BT at a reaction temperature of 310 °C. Pt to LOHC-ratio of 1/57135, powder catalyst < 250 μm, 4 – 5.2 bara and stirring rate of 1000 1/min.

Table 1
Estimated parameters of the intrinsic kinetic model to describe the ground powder catalyst.

$k_{0,1}$	7.13e8	$\mathrm{L}^{a1}\,\mathrm{g_{kat}^{-1}}\,\mathrm{mol_{H12}}^{-a1+1}\,\mathrm{bar}^{-a2}\,\mathrm{s}^{-1}$
$E_{A,1}$	149.72	$\mathrm{kJ\,mol}^{-1}$
$a1$	2.08	–
$a2$	− 0.53	–
$k_{0,2}$	2.68e8	$\mathrm{L}^{b1}\,\mathrm{g_{kat}^{-1}}\,\mathrm{mol_{H6}}^{-b1+1}\,\mathrm{bar}^{-b2}\,\mathrm{s}^{-1}$
$E_{A,2}$	141.39	$\mathrm{kJ\,mol}^{-1}$
$b1$	1.8e-6	–
$b2$	− 0.8	–

in previous work [14]. Because a lower activation energy indicates mass transfer limitations, we hypothesize that the high activation energy found in our study is a further clear indication of the intrinsic nature of the here-determined reaction rates. H12-BT dehydrogenation is found to be strongly affected by the concentration of H12-BT as shown by the reaction order a1 of around 2. The reduced activity with increasing hydrogen partial pressure results in a reaction order regarding hydrogen a2 of close to −0.5. H6-BT dehydrogenation seems to be almost independent on H6-BT concentration with b1 being determined with a value close to 0. However, the reverse reaction is dependent on H6–BT concentration and so is the overall reaction rate. H6-BT dehydrogenation is negatively influenced by increasing hydrogen partial pressure as the reaction order for hydrogen b2 is −0.8.

Fig. 6 compares the regressed and experimentally determined concentrations to evaluate the quality of the fit. In most cases the deviation between experimental and calculated values is below 20 %, indicating that the kinetic model is suitable for describing the major effects of the process parameters on the formation and consumption rates of H12-BT,
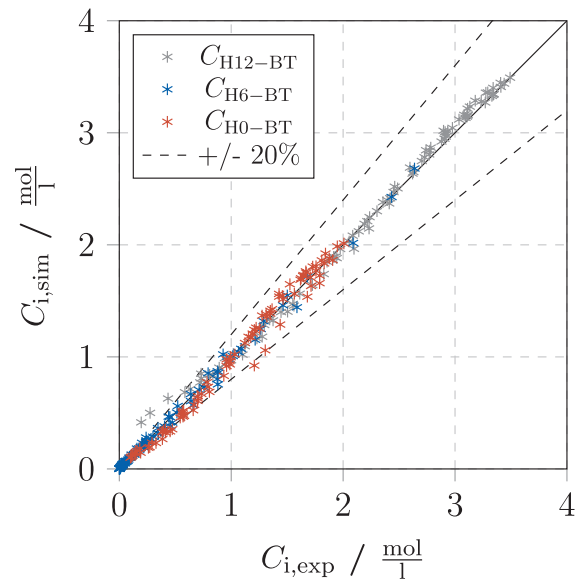

Fig. 6. Parity diagram comparing the experimentally determined and regressed concentrations obtained *from the developed kinetic model based on experimental data with the ground powder catalyst.*

H6-BT and H0-BT, respectively. Furthermore, no systematic deviations are observed. The quality of the fit is also emphasized by a high adjusted coefficient of determination R^2_{adj} of 0.992.

3.4. Effective reaction rate using commercial catalyst pellets

While our batch experiments with the milled catalyst were designed to ensure intrinsic kinetics free from any mass transport influence, the operation of a H12-BT dehydrogenation reaction in a continuous fixed-bed tubular reactor requires a careful re-examination of such potential limitations. A milled catalyst would cause a too high pressure drop in a continuously operated fixed-bed reactor and thus a pellet catalyst needs to be used in continuous operation. External mass transfer limitations can be excluded by choosing sufficient flow rates of the reactants and a proper reactor design. Internal mass transfer limitations cannot be influenced by flow rates or reactor design for a given pellet catalyst. As the catalyst needs to be used in its original shape, the estimation of kinetic parameters for the pellet catalyst is required for the design of a continuously operated fixed-bed reactor using the commercially available catalyst. The synthesis of a new catalyst with increased pore size would be an option to improve internal mass transfer while maintaining a low pressure drop. However, the proper dispersion of the Pt nanoparticles requires a certain range of support pore sizes.

In this light we were interested to investigate next to the milled catalyst also the commercial pellet catalyst in its original state to determine a kinetic model for its effective hydrogen release rate. Our intension is to compare the intrinsic and the effective reaction rates in order to determine the optimization potential through catalyst design, e. g. by developing targeted modifications of the catalyst shape for the operation conditions of interest. Our experiments for the parameter estimation for the effective kinetic approach have been carried out at temperature between 280 °C and 320 °C and the pressure between 2 and 6 bara. The found dependencies of the reaction rate on temperature and pressure are qualitatively equal to the dependencies of the intrinsic model and are summarized in the ESI (see Figs. S7, S8 and S9). The same kinetic approach and the same procedure as described above were used to estimate the parameters for the effective H12-BT dehydrogenation kinetics. The estimated parameters are given in Table 2.

The determined activation energy for both reactions (H12-BT to H6-BT and H6-BT to H0-BT) is between 110 and 115 kJ mol^{-1}. This lower value is expected and reflects the internal mass transfer effect on the temperature dependency of the reaction rate. Noticeably, the reaction order b1,eff is significantly higher than in the intrinsic approach. All other estimated reaction orders are lower in the effective kinetic approach than in the intrinsic approach. Fig. 7 shows the parity plot of the regressed and measured concentrations of H12-BT, H6-BT and H0-BT. The deviation is mostly below 20 % and no systematic deviation can be detected. The adjusted coefficient of determination R^2_{adj} is 0.994 and confirms the high quality of the fit.

3.5. Catalyst utilization

The catalyst utilization η is defined as the ratio of the effective reaction rate and the intrinsic reaction rate for a given set of process parameters (see Eq. (6). The catalyst utilization η is calculated using the effective and intrinsic approach related to the catalyst mass with the corresponding parameters given in Tables 1 and 2. A high catalyst utilization is desired to make maximum usage of the expensive precious
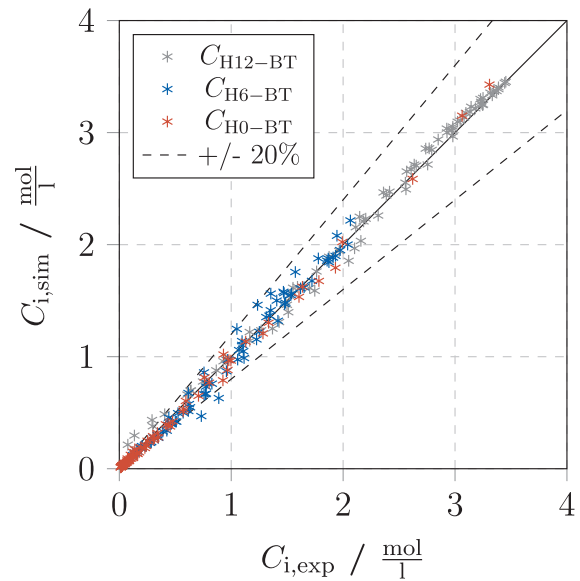

Fig. 7. Parity diagram comparing the experimentally determined and regressed concentrations *obtained from the kinetic model for the H12-BT dehydrogenation with the pellet catalyst.*

metal in the catalyst. Based on our developed models the catalyst utilization can now be calculated for the commercial catalyst over a wide range of process conditions. The result can give guidelines for future optimization of pelletized H12-BT dehydrogenation catalysts.

$$\eta = \frac{r_{\text{eff}}}{r_{\text{int}}} \tag{6}$$

Fig. 8 shows the estimated catalyst utilization for the pressure range between 2 and 5 bara total pressure and temperatures between 270 °C and 345 °C. This parameter range is highly relevant for the technical use of the liquid phase H12–BT/H6-BT dehydrogenation. The catalyst utilization is calculated for H12-BT and H6-BT dehydrogenation. The reaction rate for H12-BT dehydrogenation is calculated for a H12-BT conversion of 2.5 %. The reaction rate of H6-BT dehydrogenation is determined up to a H0-BT yield of 2.5 %. Both selections have been made to calculate the effectiveness factor at the highest relevant system activity.

As expected, the catalyst utilization decreases with rising temperature as the surface reaction is strongly, and the mass transfer rate is only mildly dependent on temperature. Catalyst utilization increases with rising hydrogen partial pressure and rising total pressure. In general, the catalyst utilization is below 50 % with the tested commercial catalyst despite the fact that this catalyst material is characterized by an egg-shell impregnation to mitigate internal diffusion limitation. Thus, our results indicate that catalyst utilization could be increased if the thickness of the egg-shell layer would be reduced, or the pore diameter of the support material would be further increased. This information is very relevant for future catalyst optimization studies.

The data from the results section of this publication are also available via Zenodo [39].

4. Conclusion

In this publication, the dehydrogenation of H12-BT in the liquid phase has been investigated in detail using a commercially available catalyst. For the first time, a kinetic approach has been developed that considers the consecutive nature of the reaction involving both the dehydrogenation of H12-BT to H6–BT and the dehydrogenation of H6-BT to H0-BT and thermodynamic limitation. Furthermore, the pressure dependency of liquid phase H12-BT dehydrogenation was

Table 2
Estimated parameters of the kinetic model developed to describe the effective kinetics with the commercial pelletized catalyst in its original shape.

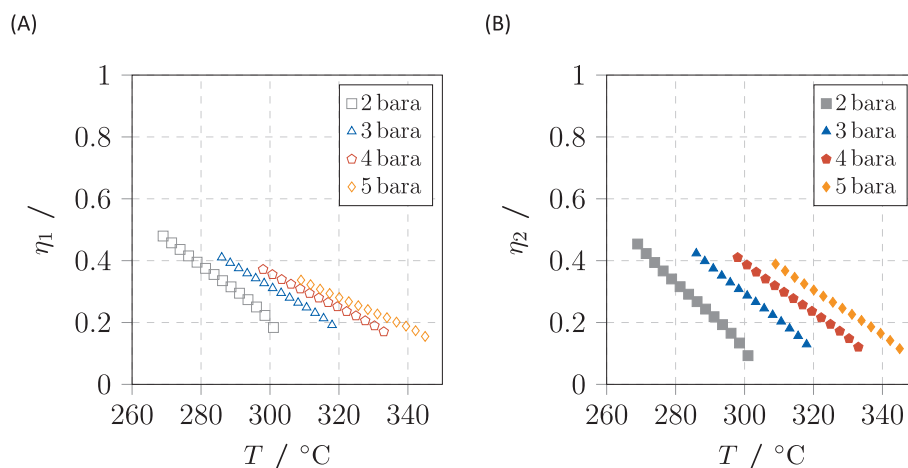|		
$k_{0,1,eff}$	1.73e5	L^{a1,eff} g$_{kat}^{-1}$ mol$_{H12}^{-a1,eff+1}$ bar$^{-a2,eff}$ s^{-1}
$E_{A,1,eff}$	112.41	kJ mol^{-1}
a1,eff	1.53	–
a2,eff	−0.33	–
$k_{0,2,eff}$	6.67e4	L^{b1,eff} g$_{kat}^{-1}$ mol$_{H6}^{-b1,eff+1}$ bar$^{-b2,eff}$ s^{-1}
$E_{A,2,eff}$	107.58	kJ mol^{-1}
b1,eff	0.16	–
b2,eff	−0.37	–

(A)

(B)

Fig. 8. Calculation of the catalyst utilization according to Eq. (6), using the kinetic models from Eqs. (4) and (5) in the temperature range between 270 °C and 350 °C and at total pressures between 2 and 5 bara. Figure A shows η_1, which describes the catalyst utilization for the dehydrogenation of H12-BT to H6-BT. Figure B shows η_2, which describes the catalyst utilization for the dehydrogenation of H6-BT to H0-BT.

investigated in detail and considered in the kinetic approach.

First, the intrinsic kinetics of the reaction were investigated by strictly excluding mass transfer influences through external and internal diffusion. This was realized by sufficient stirring in the applied batch dehydrogenation reactor and using milled catalyst particles. It was found that external mass transfer influences can be excluded under the applied conditions. While the commercial pellet catalyst with a pellet size of around 3 mm was found to be limited by internal mass transport, grinding of the pellets to smaller than 500 μm proved effectively to prevent pore diffusion limitation.

Based on the experimental data collected for reactions free of mass transfer influences, expressions for the intrinsic kinetics of H12-BT and H6-BT dehydrogenation were developed. For this purpose, a power law approach that considers limitation of the thermodynamic equilibrium has been applied. The kinetic parameters were estimated for the intrinsic reaction rate. Subsequently, effective kinetic data for the technical catalyst pellets under internal mass transfer limitation were collected in the same way followed by parameter estimation for this technically very relevant case. For both cases, intrinsic and effective kinetics, the reaction rates can be predicted with the developed model in a high accuracy with coefficients of determination above 0.99. This underscores the suitability of the developed kinetic approach as a basis for creating a reactor model that can be used to evaluate LOHC-based on board hydrogen supply in mobile applications. By comparing the calculated intrinsic and effective reaction rates, a catalyst utilization factor can be calculated. All calculated effectiveness factors were below 0.5 which shows that the utilization of the commercial pelletized catalyst leaves still a lot of room for further optimization, for example, by adapting the pellet size and pellet shape to the specific requirements of the H12-BT dehydrogenation reaction.

CRediT authorship contribution statement

T. Mader: Writing – original draft, Visualization, Validation, Software, Methodology, Investigation, Formal analysis, Data curation. **M. Blasius:** Writing – review & editing, Validation, Methodology, Formal analysis. **S. Pappler:** Writing – review & editing, Validation, Methodology, Formal analysis. **T. Rüde:** Writing – review & editing, Validation, Methodology. **M. Geißelbrecht:** Writing – original draft, Supervision, Resources, Project administration, Methodology, Formal analysis, Conceptualization. **P. Wasserscheid:** Writing – review & editing, Supervision, Resources, Project administration, Methodology, Funding acquisition, Conceptualization.

Declaration of competing interest

The authors declare that they have no known competing financial interests or personal relationships that could have appeared to influence the work reported in this paper.

PW is co-founder and minority shareholder of Hydrogenious LOHC Technologies GmbH, Erlangen, a company that has commercialized equipment for hydrogen storage using the LOHC technology.

Acknowledgements

Appendix A. Supplementary data

Supplementary data to this article can be found online at https://doi.org/10.1016/j.fuel.2025.136928.

Data availability

Data available on Zenodo

References

[1] Preuster P, Alekseev A, Wasserscheid P. Hydrogen storage technologies for future energy systems. Annu Rev Chem Biomol Eng 2017;8:445–71. https://doi.org/10.1146/annurev-chembioeng-060816-101334.

[2] Rüde T, Dürr S, Preuster P, Wolf M, Wasserscheid P. Benzyltoluene/perhydro benzyltoluene – pushing the performance limits of pure hydrocarbon liquid organic hydrogen carrier (LOHC) systems. Sustainable Energy Fuels 2022;6(6):1541–53. https://doi.org/10.1039/d1se01767e.

[3] M.-J. Zhou, Y. Miao, Y. Gu, and Y. Xie, "Recent Advances in Reversible Liquid Organic Hydrogen Carrier Systems: From Hydrogen Carriers to Catalysts," Advanced materials (Deerfield Beach, Fla.), early access. doi: 10.1002/adma.202311355.

[4] Distel MM, et al. Large-scale H 2 storage and transport with liquid organic hydrogen carrier technology: insights into current project developments and the future outlook. Energy Tech 2024:2301042. https://doi.org/10.1002/ente.202301042.

[5] Staudt C, et al. Process engineering analysis of transport options for green hydrogen and green hydrogen derivatives. Energy Tech 2024:2301526. https://doi.org/10.1002/ente.202301526.

[6] Biswas S, Moreno Sader K, Green WH. Perspective on decarbonizing long-haul trucks using onboard dehydrogenation of liquid organic hydrogen carriers. Energy Fuels 2023;37(22):17003–12. https://doi.org/10.1021/acs.energyfuels.3c01919.

[7] Regele C, Gackstatter F, Ortner F, Preuster P, Geißelbrecht M. Simulation and optimization of a liquid organic hydrogen carrier based hydrogen train system. Energ Conver Manage 2025;344:120234. https://doi.org/10.1016/j. enconman.2025.120234.

[8] D. Acharya, D. Ng, and Z. Xie, "Recent Advances in Catalysts and Membranes for MCH Dehydrogenation: A Mini Review," Membranes, early access. doi: 10.3390/membranes11120955.

[9] Alhumaidan F, Cresswell D, Garforth A. Hydrogen storage in liquid organic hydride: producing hydrogen catalytically from methylcyclohexane. Energy Fuels 2011;25(10):4217–34. https://doi.org/10.1021/ef200829x.

[10] Sinfelt JH, Hurwitz H, Shulman RA. Kinetics of methylcyclohexane dehydrogenation over PT—Al 2 O 3. J Phys Chem 1960;64(10):1559–62. https://doi.org/10.1021/j100839a054.

[11] Geißelbrecht M, Benker R, Seidel A, Preuster P. Modeling of the continuous dehydrogenation of perhydro-dibenzyltoluene in a cuboid reactor. Energy Tech 2024:2300813. https://doi.org/10.1002/ente.202300813.

[12] Willer M, Preuster P, Geißelbrecht M, Wasserscheid P. Continuous dehydrogenation of perhydro benzyltoluene and perhydro dibenzyltoluene in a packed bed vertical tubular reactor – the role of LOHC evaporation. Int J Hydrogen Energy 2024;57:1513–23. https://doi.org/10.1016/j.ijhydene.2024.01.031.

[13] Jorschick H, Dürr S, Preuster P, Bösmann A, Wasserscheid P. Operational stability of a LOHC-based hot pressure swing reactor for hydrogen storage. Energy Tech 2019;7(1):146–52. https://doi.org/10.1002/ente.201800499.

[14] Wang Q, et al. Investigation on catalytic distillation dehydrogenation of perhydro-benzyltoluene: reaction kinetics, modeling and process analysis. Chem Eng J 2024; 482:148591. https://doi.org/10.1016/j.cej.2024.148591.

[15] Kadar J, et al. Boosting power density of hydrogen release from LOHC systems by an inverted fixed-bed reactor design. Int J Hydrogen Energy 2024;59:1376–87. https://doi.org/10.1016/j.ijhydene.2024.02.096.

[16] Y. Mahayni, L. Maurer, I. Baumeister, F. Auer, P. Wasserscheid, and M. Wolf, Batch and continuous synthesis of well-defined Pt/Al2O3 catalysts for the dehydrogenation of homocyclic LOHCs, 2024.

[17] Bong B, Mebrahtu C, Jurado D, Bösmann A, Wasserscheid P, Palkovits R. Hydrogen loading and release potential of the LOHC system Benzyltoluene/Perhydro Benzyltoluene over S–Pt/TiO 2 Catalyst. ACS Eng Au 2024: acsengineeringau.4c00003. https://doi.org/10.1021/acsengineeringau.4c00003.

[18] Auer F, Solymosi T, Erhardt C, Collados CC, Thommes M, Wasserscheid P. Enhancing the power density of hydrogen release from LOHC systems by high Pt loadings on hierarchical alumina support structures. Int J Hydrogen Energy 2025; 100:1282–90. https://doi.org/10.1016/j.ijhydene.2024.12.155.

[19] Strauch D, et al. Bimetallic platinum rhenium catalyst for efficient low temperature dehydrogenation of perhydro benzyltoluene. Cat Sci Technol 2024;14(7):1775–90. https://doi.org/10.1039/d3cy01336g.

[20] Auer F, et al. Boosting the activity of hydrogen release from liquid organic hydrogen carrier systems by sulfur-additives to Pt on alumina catalysts. Cat Sci Technol 2019;9(13):3537–47. https://doi.org/10.1039/C9CY00817A.

[21] Bong B, Kopp WA, Nevolianis T, Mebrahtu C, Leonhard K, Palkovits R. Reaction equilibria in the hydrogen loading and release of the LOHC System Benzyltoluene/ Perhydro Benzyltoluene. Chem Eng & Technol 2025:e12002. https://doi.org/ 10.1002/ceat.12002.

[22] S. Park, M. Naseem, and S. Lee, "Experimental Assessment of Perhydro-Dibenzyltoluene Dehydrogenation Reaction Kinetics in a Continuous Flow System for Stable Hydrogen Supply," Materials (Basel, Switzerland), early access. doi: 10.3390/ma14247613.

[23] Geißelbrecht M, Mrusek S, Müller K, Preuster P, Bösmann A, Wasserscheid P. Highly efficient, low-temperature hydrogen release from perhydro-benzyltoluene using reactive distillation. Energy Environ Sci 2020;13(9):3119–28. https://doi. org/10.1039/d0ee01155j.

[24] Dürr S, et al. Experimental determination of the hydrogenation/dehydrogenation - Equilibrium of the LOHC system H0/H18-dibenzyltoluene. Int J Hydrogen Energy 2021;46(64):32583–94. https://doi.org/10.1016/j.ijhydene.2021.07.119.

[25] Rüde T, et al. Performance of continuous hydrogen production from perhydro benzyltoluene by catalytic distillation and heat integration concepts with a fuel cell. Energy Tech. 2023;11(3):2201366. https://doi.org/10.1002/ ente.202201366.

[26] Henseler J, Schärfe T, Steffen J, Görling A, Geißelbrecht M, Wasserscheid P. Detailed analysis of coke precursor formation in catalytic perhydro benzyltoluene dehydrogenation processes. Fuel 2025;398:135500. https://doi.org/10.1016/j. fuel.2025.135500.

[27] Jorschick H, et al. Hydrogen storage using a hot pressure swing reactor. Energy Environ Sci 2017;10(7):1652–9. https://doi.org/10.1039/c7ee00476a.

[28] Willer M, Preuster P, Malgaretti P, Harting J, Wasserscheid P. Heat transfer to a catalytic multiphase dehydrogenation reactor. Int J Hydrogen Energy 2024;80: 1011–20. https://doi.org/10.1016/j.ijhydene.2024.07.073.

[29] Heublein N, Stelzner M, Sattelmayer T. Hydrogen storage using liquid organic carriers: Equilibrium simulation and dehydrogenation reactor design. Int J Hydrogen Energy 2020;45(46):24902–16. https://doi.org/10.1016/j. ijhydene.2020.04.274.

[30] Stephen E. Stein, and Robert L. Brown, "Structures and Propeties Group Additivity Model in NIST Chemistry WebBook, NIST Standard Reference Database Number 69, Eds. P.J. Linstrom and W.G. Mallard," National Institute of Standards and Technology, Gaithersburg MD, doi: 10.18434/T4D303. Accessed: Jul. 30, 2025.

[31] Verevkin SP, Vostrikov SV, Leinweber A, Wasserscheid P, Müller K. Thermochemical properties of benzyltoluenes and their hydro- and perhydro-derivatives as key components of a liquid organic hydrogen carrier system. Fuel 2023;335:126618. https://doi.org/10.1016/j.fuel.2022.126618.

[32] Jorschick H, Geißelbrecht M, Eßl M, Preuster P, Bösmann A, Wasserscheid P. Benzyltoluene/dibenzyltoluene-based mixtures as suitable liquid organic hydrogen carrier systems for low temperature applications. Int J Hydrogen Energy 2020;45 (29):14897–906. https://doi.org/10.1016/j.ijhydene.2020.03.210.

[33] Eastman. "Marlotherm® LH heat transfer fluid product guide." Accessed: Apr. 24, 2025. [Online]. Available: https://www.eastman.com/content/dam/eastman/cor porate/en/literature/s/sfehtf10985.pdf.

[34] Bulgarin A, Jorschick H, Preuster P, Bösmann A, Wasserscheid P. Purity of hydrogen released from the Liquid Organic Hydrogen Carrier compound perhydro dibenzyltoluene by catalytic dehydrogenation. Int J Hydrogen Energy 2020;45(1): 712–20. https://doi.org/10.1016/j.ijhydene.2019.10.067.

[35] Madon RJ, Boudart M. Experimental criterion for the absence of artifacts in the measurement of rates of heterogeneous catalytic reactions. Ind Eng Chem Fund 1982;21(4):438–47. https://doi.org/10.1021/i100008a022.

[36] A. Wunsch, M. Mohr, and P. Pfeifer, "Intensified LOHC-Dehydrogenation Using Multi-Stage Microstructures and Pd-Based Membranes," Membranes, early access. doi: 10.3390/membranes8040112.

[37] Koschany F, Schlereth D, Hinrichsen O. On the kinetics of the methanation of carbon dioxide on coprecipitated NiAl(O). Appl Catal B 2016;181:504–16. https:// doi.org/10.1016/j.apcatb.2015.07.026.

[38] Usman MR, Cresswell DL, Garforth AA. Dehydrogenation of Methylcyclohexane: parametric Sensitivity of the Power Law Kinetics. ISRN Chem Eng 2013;2013:1–8. https://doi.org/10.1155/2013/152893.

[39] T. Mader, M. Blasius, S. Pappler, T. Schärfe, M. Geißelbrecht, and P. Wasserscheid, "Dataset for Development of a Kinetic Approach for the Liquid Phase Dehydrogenation of Perhydro Benzyltoluene,". 2025. doi: 10.5281/ zenodo.16561666.